Quantification of land-sea nutrient fluxes supplied by allis shad across the species' range

Camille Poulet, Betsy Barber-O'Malley, Géraldine Lassalle, Patrick Lambert

Quantification of land-sea nutrient fluxes supplied by allis shad across the species' range

Camille Poulet[**], Betsy L. Barber-O'Malley [1,2,†], Géraldine Lassalle[1] and Patrick Lambert[1]

[1]: INRAe, UR EABX, 50 Avenue de Verdun, 33612 Cestas Cedex, France

[2]: University of Maine, 168 College Avenue, Orono, ME 04469, United-States

Competing interests statement: The authors declare there are no competing interests.

[*] corresponding author: camille.poulet@inrae.fr
Phone: +33 (0)5 57 89 08 00

[†] Present address : Present address: Gomez and Sullivan Engineers, 41 Liberty Hill Road, Henniker, NH 03242, USA

Abstract

Diadromous species act as nutrient vectors between their marine and freshwater habitats. Few valuations of this regulating service exist and none at the scale of species distribution ranges. This large-scale approach seems particularly relevant for species moving and exchanging individuals across borders and territories as these populations may strongly depend upon each other in terms of population viability and provision of ecosystem services. The development of a new nutrient routine within an existing mechanistic species distribution model provided estimates of the 'maximum potential' of the anadromous allis shad (*Alosa alosa*) to provide nitrogen and phosphorous subsidies throughout Western Europe. During their seasonal reproductive migration, shad provided low amounts of nutrient subsidies when compared to North-American anadromous species and annual riverine nutrient loads. However, these subsidies are delivered as pulses concentrated in space and time, suggesting that more work is needed to figure out the significance of these shad-derived nutrients in terms of riverine ecosystem functioning. The evidence of a substantial flow of strayers delivering nutrient subsidies in several rivers confirmed the need for large-scale management of migratory species to ensure a sustainable provision of ecosystem services.

Keywords: regulating services, nutrient subsidies, dispersal, allis shad, distribution scale

Introduction

Diadromous species (land-sea migrating fishes) are cross-border resources: they move between fresh and marine waters to complete their life cycles (McDowall 1988), and population exchange can occur among river basins in different territories and administrative boundaries. Given this complex life cycle, diadromous species have been adversely affected by multiple human activities (e.g. overexploitation, degradation of essential habitats, losses of connectivity, pollution, water withdrawal, climate change). These cumulative pressures led to a generalized decline in abundances across their distribution ranges with drastic losses of associated services provided to local human communities (Limburg and Waldman 2009; Wilson and Veneranta 2019). In terms of provisioning services, diadromous species have been targeted by commercial fisheries over centuries and across continents and are highly prized in aquaculture food production (Kobayashi et al. 2015). They were recognized as one of the major protein and bioavailable micronutrient sources for human communities across the world (Hicks et al. 2019). For example, Salmonidae contain high percentages of fatty acids essential to human health (Joordens et al. 2014). Diadromous species also provide cultural services, and are historically prevalent in cultural practices (e.g. brotherhoods and ceremonies), gastronomy, diet, medicines and material items (e.g. Bolster (2008)). Some of these species are described as charismatic, emblematic, and iconic (i.e. cultural keystone species census (Garibaldi and Turner 2004)). The relative importance of the cultural services associated with diadromous species is suspected to be growing over time in relation with the global rarefaction of fish populations (Drouineau et al. 2018). As an example, in Sweden, Haro (2009) reported a massive shift from commercial to recreational fisheries due to a declining trend in fish abundances. Consequently, recreational fishing has gradually become a high-value recreational activity across the Baltic region and elsewhere (Hyder et al. 2018).

Besides their well-known significance in terms of provisioning and cultural services, diadromous species have also been recognized as strong ecological drivers for major biological cycles because of their role as nutrient 'conveyor belts'. In particular, anadromous species (which migrate from marine habitats to upstream rivers to spawn (McDowall 1988)) accumulate substantial amounts of embodied marine nutrients during their growing phase at sea. These marine-derived nutrients are moved from the ocean into freshwater habitats through migrations and may positively affect estuarine and riverine ecosystem functioning. Of central significance are the semelparous anadromous species (fishes dying after reproduction). After spawning, decomposing carcasses provide a consistent and bioavailable source of nutrients for freshwater communities and food webs at multiple trophic levels (Samways et al. 2015, 2018; Twining et al. 2017). In particular, nutrient enrichment from carcasses increases the overall primary productivity (Durbin et al. 1979), the biomass of biofilm algae and fungi, the bacteria density (Samways and Cunjak 2010), and modifies the macroinvertebrates assemblages at local scale (Guyette et al. 2014; Weaver et al. 2018). Increases in growth and survival of juveniles salmonids were also observed in streams receiving adult salmon subsidies, providing evidence for a positive feedback loop (Bilby et al. 1996; Wipfli et al. 2003; Scheuerell et al. 2005) with suspected evolutionary consequences at the species level (Auer et al. 2018).

Despite being a widely recognized process, quantitative estimates of these regulating services are still scarce, and mainly concern Pacific salmon (*Oncorhynchus* spp) runs in North America. Pacific salmon-derived nutrients are released through the metabolism of spawning fish in the form of excretion and the decay of spawners' carcasses (Naiman et al. 2002; Schindler et al. 2003). In the Columbia River, Gresh et al. (2000) estimated that Pacific salmons historically contributed over 3,000 metric tons of nitrogen (N) and 360 metric tons of phosphorus (P) each year. Similarly to salmon from the U.S. Pacific coast, is the case of

alosines (i.e. blueback herring *(Alosa aestivalis*) and alewife (*Alosa pseudoharengus*) that used to provide large quantities of marine-derived nutrients throughout their native range along the U.S. Atlantic coast (Durbin et al. 1979; Garman 1992; West et al. 2010). These previous works gave critical insights on the ecological roles of diadromous species in the nutrient status of river basins, particularly upper reaches. However, these studies were mostly catchment-specific and were only performed in a limited number of locations throughout the Eastern U.S. coast. Although migratory species produce and deliver ecosystem services locally, the dynamics of the species is often triggered by the spatial distribution of resources and thereby depend on habitats that are isolated spatially from the places where services are provided (Kremen et al. 2007). Thus, the supplies received by society from a migratory species are relying on favorable habitats encountered by the species in other parts of the range. On that, "spatial mismatches" are likely to occur between areas where species "provided the most ecosystem services" and those that "support population ability" to provide sustainable services (Semmens et al. 2011, 2018; MEA, 2005). For diadromous species that migrate over long distances, 'spatial mismatches' can occur within the same country, region, or states or far beyond political boundaries, leading to consider multiple spatial scales, from regional to inter-state, to find the most relevant one for conservation issues. Thus, having estimates of the nutrient subsidies translocated by shads at the scale of the distribution range in catchments for which no data were available is of particular relevance. Assessments and management of ecosystem services linked to diadromous species required consideration of larger spatial scales, and specific methods for estimating the extent to which distinct locations benefit or support the provision of ESs between them. Such challenge requires an explicit consideration of fish movement and their magnitude. So that, estimations of services explicitly including metapopulation dynamics and dispersal seem vital to address this management and conservation challenge (López-Hoffman et al. 2010).

In Europe, allis shad (*Alosa alosa*) populations have experienced a persistent and significant decline across their range (ICES 2015). Overfishing, water pollution, dam construction, habitat degradation, and more recently, invasive species can be held responsible for such a decrease (Limburg and Waldman 2009). In the Gironde-Garonne-Dordogne system (GGD) in France, known as the largest allis shad population in Europe, spawning runs of almost 400 0000 fish migrating upstream in the 80's have drastically declined to only thousands of fish at the end of the 20th century (Baglinière and Élie 2000; Castelnaud et al. 2001). Similar to the GGD, annual catches of shad in the Minho River (Spain-Portugal) decreased by about 90% after the 50's (Mota et al. 2016). Therefore, the species was listed on the Red List of the International Union for the Conservation of Nature (IUCN) and benefits from regional conservation status. Despite this overall decline, allis shad populations in 'reference' basins in France, Spain, and Portugal are still considered of high cultural and ecological value, confirming the need for innovative scientific insights and perspectives to enhance management efforts at both local and global scales (see https://diades.eu).

In this context, the aim of this study was to provide the first quantification of nutrient imports and exports delivered by shad populations across its distribution range with explicit consideration of connections among different river basins. The case study of allis shad in Western Europe over the early 20th century was considered. A mechanistic species distribution model called G3RD (Global Repositioning Dynamics of Diadromous fish Distribution) was developed for any anadromous species and was first parameterized for allis shad (Rougier et al. 2014, 2015). The model was first used to assess the species range-shift response to the thermal component of climate change, suggesting that allis shad may be able to cope successfully with ongoing climate change that should not be perceived as a major threat to the species long-term persistence (Rougier et al., 2015). Integrating temperature was the most straightforward way to address the climate change issue on fish, given their

ectothermic nature. Based on the existing literature, three life cycle processes, i.e. including growth at sea (Gilligan-Lunda et al. 2021), survival of spawners (Paumier et al. 2019), and survival of early-life stages in rivers (Jatteau et al. 2017), were linked to temperature to account for whole-life cycle impacts to global warming (Rougier et al. 2014). To assess the potential for shad to deliver nutrients across European river basins, an original nutrient routine providing estimates of nutrient imports and exports was designed and combined with GR3D. This study focused on evaluating the interdependences between river basins in the provision of nutrients subsidies in the context of metapopulation dynamics demonstrated for shad (Martin et al. 2015; Randon et al. 2018).

Material and Methods

A brief description of the GR3D model and the key updates to improve and test the overall model robustness are provided in sections 1 and 2. The new routine added to GR3D to quantify nutrient fluxes is presented in section 3. The updated code is available online at https://github.com/inrae/GR3D/tree/v3.2.1 and http://doi.org/10.5281/zenodo.4442030. For a more detailed description of the GR3D model, see Appendix 1 or Rougier (2014) and Rougier et al. (2014).

1. GR3D model presentation and main improvements

1.1. Population dynamics within the model

GR3D is an individual-based stochastic model. It explicitly combines population dynamics with key life cycle events and climatic requirements. The GR3D model was written in Java using the 'SimAqualife' software framework specifically designed for spatialized and individual-based simulations to explore the movements of aquatic species (Dumoulin 2007). The model covers the entire anadromous life cycle and is divided into six sub-models depicting the key events, including (i) reproduction, (ii) growth, (iii) survival, (iv) downstream migration, (v) maturation, and (vi) dispersal and upstream migration (Figure 1). A set of 42 parameters obtained from the primary literature, expert elicitation, or model calibration was used to define these different processes. Most of the data used in GR3D came from the Garonne River in the South-West of France, which was considered as a 'reference' population for shad in Europe (for more details, see Rougier et al. (2014) and Rougier et al. (2015))(Table A1 and Fig. A1). Three life cycle processes, including growth at sea, survival of spawner before they reproduce, and survival of early-life stages in rivers, were linked to water temperature, as further described.

169 The "physical" environment of GR3D was divided into "two worlds": the continental and
170 marine compartments, which are split into a set of 'river basins' and 'sea basins', respectively.
171 River and sea basins are connected to each other and spatially geo-referenced. This "physical"
172 environment represents the European Atlantic coast from the south of Portugal to the British
173 Isles and Norway that covers the core distribution of the species (Fig. A1). River and sea
174 basins are both characterized by seasonal temperature time series (T°C), while river basins are
175 also characterized by their surface area (km^2) and geographic position (latitude and longitude
176 at the river mouth).

177 Fish progressed through the life cycle with a seasonal time step. Reproduction
178 occurred every spring in all rivers when spawners were present. The number of recruits
179 produced by the spawning stock in river basin *j* was modeled as a density-dependent process
180 using a Beverton and Holt stock-recruitment relationship (BH-SR) (Beverton and Holt
181 1957)(Figure 1 and eq1.(A1)). Egg production in basin *j* was linked to species fecundity (α)
182 and the number of spawners present. The BH-SR relationship was modeled so that recruit
183 mortality was dependent on both temperature and basin size to consider resource limitations
184 in small basins. The relationship between recruit mortality and temperature follows a dome-
185 shaped curve (Rosso et al. 1995), with the number of recruits decreasing when temperature is
186 below or above an optimal value. The tolerance and optimal thermal ranges are defined as
187 model parameters (Table A1). An 'Allee effect' (Stephens et al. 1999), proportional to the
188 river basin size, was also integrated into the stock-recruitment relationship to prevent the
189 formation of a functional population from only a limited number of individuals settling in a
190 river basin.

191 In early summer, juveniles migrated from their upstream habitats through rivers and
192 estuaries to reach the associated sea basin in the physical environment where they could grow
193 and sexually mature. Fish growth was modeled using a Von Bertalanffy growth function (Von

Bertalanffy 1938) (eq2. (A1)). Since temperature is known to affect growth rate, a dome-shaped curve, similar to the one for reproduction, was used to link the growth coefficient (K, defined as a model parameter, Table A1) to water temperature and introduce seasonal and in-river variability on fish growth (Rosso et al. 1995; Kielbassa et al. 2010; Bal et al. 2011).

After spending several years at sea, ripe individuals started their spawning migration and entered a river basin to reproduce. An individual was assumed to be mature when it reached its size at maturity, L_{mat}, defined as a model parameter (Table A1).

Dispersal from the ocean to a given river basin occurred in three main steps: emigration, transfer, and settlement. Emigration depended on whether individuals adopted a homing behavior (i.e. individuals return to their natal river to reproduce) or a straying behavior (individuals colonize a new river basin that differs from their natal origin to reproduce). The probability of adopting a homing behavior (P_{hom}) was considered as a specific life-history trait and hence did no vary among populations. Consequently, the probability of adopting a straying behavior (1- P_{hom}) was imposed to be the same for all rivers considered in this study. During the transfer phase, individuals adopting a homing behavior simply enter the natal river to spawn. For strayers, the probability of entering a new river basin in the physical environment was linked to the distance separating the new river basin from the natal river. Then, relatively to the pairwise distances, a weight was assigned to each river basin using a logit function with most parameters defined as model parameters (see Table A1 and eq3. (A1) for more details). All the weights were then standardized so that the sum of weights equaled 1 providing the probability for each river basin to be selected. Migrating spawners then entered the specific river basin, survived, and reproduced if they found suitable thermal conditions.

At each time step, the probability of survival for each individual was estimated using its location along the land-sea continuum. The seasonal survival probability accounted for annual mortality coefficients at sea and in the river, with the latter depending on the water

219 temperature. After reproduction, the probability of survival for spawners was defined by the
220 Sp_{sp} parameter. As allis shad is a semelparous species and the majority of individuals die after
221 reproduction, the probability of survival was set to a low value of 0.1 (Table A1). Most
222 individuals died after reproduction, with their carcasses remaining in the river to decompose.
223 Surviving spawners returned to the sea to reproduce the following years.
224
225 1.2. Sex differentiation and main improvements of the GR3D model
226 The amounts of nitrogen (N) and phosphorus (P) brought by shads into river systems can
227 vary depending on sex because males and females differ in their elemental composition and
228 mass-at-age (Durbin et al. 1979; Taverny 1991). To address this, GR3D was updated to
229 estimate male and female abundances separately. Based on previous studies addressing allis
230 shad population dynamics (Mennesson-Boisneau 1990; Mennesson-Boisneau et al. 2000),
231 three parameters appeared relevant to differentiate males and females in the model: the
232 optimal growth coefficient ($K_{optGrow}$), the asymptotic length (L_{∞}), and the length at maturity
233 (L_{mat}) (Table A1). The values for the three parameters were directly estimated for both
234 genders using a non-linear optimization performed with R studio software (R Core Team
235 2018) so that the set of parameters best fits the observations of age and length. The
236 differentiation between males and females in GR3D required a doubling of the previous value
237 used for the fecundity parameter (α) in the BH-SR relationship that had only considered
238 females. When integrating both sex into the model, the number of spawners needed to reach
239 the asymptotic recruitment increased, leading to change the value of fecundity from 135 000
240 eggs to 270 000 eggs per female to keep the same BH-SR as in Rougier et al. (2014) (Table
241 A1).

Finally, the river temperature ranges ensuring recruitment and egg survival were also modified to take into account new insights on allis shad spawner and larvae thermal tolerances (Jatteau et al. 2017; Paumier et al. 2019) (Table A1).

1.3. Environmental and biological data to run simulations

Data regarding the distribution of allis shad used to run simulations were obtained from the EuroDiad 4.0 database, which records the presences and absences of European diadromous species in a total of 350 river basins throughout North Africa, Europe, and the Middle East from 1750 to present day (https://data.inrae.fr/dataset.xhtml?persistentId=doi:10.15454/IVVAIC). Based on this updated version of EuroDiad, 135 basins were integrated into the GR3D physical environment to cover the core range of the species. The major addition from Rougier et al. (2014) was the inclusion of the U.K. and Irish river basins. River basins were distributed along a latitudinal gradient from Morocco (Oum Er-Rbia (33.3°N) to Northern Scandinavia (Vefsna (65.8°N)), including the British Isles (Fig. A1). All of the 135 river basins were characterized by seasonal near-atmospheric surface temperatures at the outlet. Near atmospheric surface temperatures from 1901 to 2018 were extracted from the CRU database (https://crudata.uea.ac.uk/cru/data/hrg/#info), which consists of an atmospheric interpolated gridded dataset from weather observations with a resolution of 0.5° x 0.5°. Data were provided by the FIC (Fundación para la Investigación del Clima; https://www.ficlima.org/) as monthly means and stored as NCDF files. The 135 sea basins located in front of each river basin outlet were characterized by seasonal temperatures calculated as the mean between 12°C (temperature of the Bay of Biscay sea bottom) and the seasonal temperatures in the associated river basin.

1.4. Description of simulations

Simulations were run over the period 1800-2010 (i.e. 844 time steps). The model was initialized with an initial population set at 500 000 juveniles in each river basin. Simulations started in the summer of 1800 and were run for 100 years with constant temperature conditions (average temperatures of the 1901-1910 decade) to populate the model and limit the influence of initial conditions on simulations. Then, the model was run from 1900 to 2010 with updated seasonal temperature time-series described in section 1.3. At each time step, the model provided estimates of shad abundances in each river basin (e.g. total abundance, abundance of male and female spawners), as well as information on population status, dynamics, and spatial distribution (e.g. number of juveniles in each river basin, colonization range and number of river basins colonized). For the purpose of this study, we focused on the early 20th century, so only seasonal estimates of the first 30 years are presented in the results (i.e. 1900-1930). This period was selected because it refers to a 'pristine' situation, in which there was no clear evidence for shifts in the state and functioning of natural systems driven by human activities (also called 'the Great acceleration' of the Anthropocene (Steffen et al. 2015)). For shads, the 'pristine situation' specifically hinted that populations were still abundant and did not suffer from major human impacts or climate change. Since no anthropogenic pressures were taken into account in the GR3D model, simulation outputs corresponded to a maximum 'potential' in terms of fish and nutrients. Simulations were run until 2010 so that model estimates could be compared to observations of shad abundances, as described in the next section.

2. Partial validation of estimated fish abundances

Nutrient estimates were a function of fish abundances, so it was relevant to test the robustness of GR3D estimates. To do so, model outputs were compared to observed

abundances for a set of 13 well-studied river basins located in France, Portugal, and Spain, for which time-series of annual abundances were available (Fig. A1). Observations of shad abundances were given for different time periods depending on data availability and monitoring status of the 13 rivers. For most rivers, observations ranged from the end of the 90's to the early 2000's, with an exception for the Minho River benefiting from fisheries time series dating back to 1914. For each of the 13 rivers, annual abundances were averaged over the sampling period to be compared with abundances derived from our model from the same time range. Data regarding allis shad spawner abundance in these rivers were either derived from fisheries landings, video counting systems at fishways or based on the number of spawning events recorded at the spawning grounds ('splash-based' method). All the data and methods used to estimate observed abundances were fully described in Appendix 1.

To assess the coherence between model estimates and observed values, we classified model estimates into four categories. Rivers for which estimates were lower than observations were in 'Category 1'. Rivers for which estimates were higher than observations pertained to categories from 2 to 4 depending on how far estimates were from observations. The category number increased with the magnitude of the difference, i.e. less than two ('Category 2'), less than ten ('Category 3'), or more than ten times ('Category 4'). As no anthropogenic pressures were included in the simulations, model estimations were considered as 'validated' when the output value for a given basin was greater than the observed value but of the same order of magnitude (Categories 2 and 3).

3. Design of the nutrient routine

The amounts of nitrogen and phosphorus conveyed by shads were calculated seasonally in each of the 135 rivers through the development of a nutrient calculator implemented in the GR3D model. The routine computes nutrient loads based on the number of living and dead

316 individuals simulated each season. The net nutrient amount F_j^n provided by shads during their
317 seasonal reproductive migration in a given basin *j* was calculated as the difference between
318 the nutrient imported by migrating spawners I_j^n and nutrient exported by out-migrating
319 juveniles E_j^n (Eq. 1). The dynamics of nutrient imports provided by adults was examined in
320 the context of shad reproductive and dispersal processes. Therefore, considering a total
321 nutrient influx of N and P in the river *j*, we distinguished the contribution of fish produced by
322 the river (hereafter called 'autochthonous') from the contribution of fish coming from other
323 rivers (hereafter called 'allochthonous', see 3.3).
324

325 (1) $F_j^{n \in \{N,P\}} = \sum_{k \in \{auto,allo\}} I_{k,j}^n - E_j^n$
326

327 With "*auto"* and *"allo"* corresponding to autochthonous and allochthonous fish, respectively,
328 as presented in section 3.3.
329

330 3.1. Quantifying nutrient imports

331 Following the approaches of Haskell (2018) and Barber et al. (2018), it was assumed that
332 adults were not feeding after entering rivers in order to only account for marine-derived
333 nutrient inputs. A fish that has successfully migrated to a river after growing and maturing at
334 sea is likely to: (i) die before reaching the spawning grounds and reproducing, (ii) die after
335 reproduction (i.e. semelparous fish), or (iii) survive both reproduction and migration back to
336 the sea, (i.e. iteroparous fish). Fish that died prior to or after reproduction were considered as
337 providing the same amount of nutrient inputs. Consequently, total nutrient import, $I_{k,j}^n$,
338 corresponded to the sum of the imports from fish dying either before or after reproduction,

$Id^n_{k,j}$, and fish surviving $Is^n_{k,j}$ the reproduction season (Eq. 2) regardless of whether they were autochthonous or allochthonous:

(2) $I^n_{k,j} = Id^n_{k,j} + Is^n_{k,j}$

The main sources of nutrient inputs in river basins were assumed to be carcass decomposition, gamete emission, and fish excretion. As there was limited field data available for allis shad, carcasses inputs were computed using the average mass of male and female fish that died before spawning (Eq. 3). Gamete contribution was hence implicitly considered in the average total mass of the adults, which included both somatic and unspawned gonadic mass.

(3) $Id^n_{k,j} = \sum_{s \in \{male, female\}} Nd_{k,s,j} \times W_s \times \left(\eta^n_s + RT \times \tau^n\right)$

Where $Nd_{k,s,j}$ is either the number of male or female spawners (both autochthonous and allochthonous) that died before or after reproduction in a given river basin j, W_s is the average total mass of a male or female spawner, η^n_s is their nutrient content (% N and %P), RT is an estimate of the residence time defined as the average number of days that a fish spent in freshwater and τ^n is the excretion rate of an adult for the nutrient considered.

W was estimated for both sexes as a function of adult mean length L following the relationship $W = \alpha\ L^b$, with α and b derived from Taverny (1991)(Table 1). The original relationship was given in g.mm-^{1}, so it was converted to g.cm^{-1} (Eq.4 and Eq.4').

(4) $W_m = 4.0958 \times 10^{-3} \times L_m^{3.2252}$

(4') $W_f = 2.6654 \times 10^{-3} \times L_f^{3.3429}$

Nutrient percent contents η^n were taken from studies on American shad as no data was available for allis shad, with η_m^N = 0.02941 and η_m^P =0.00666 for males and η_f^N = 0.02958 and η_f^P =0.0067 for females (Haskell 2018). Likewise, the excretion rate τ of 2.17 × 10^{-6} µg N and 24.7171 × 10^{-5} µg P × g wet fish mass^{-1}.h^{-1} were based on results for alewife (Post and Walters 2009)(Table 1). Those values were converted in g and then multiplied by 24h to calculate a daily input. The residence time RT was assumed to be the same regardless of when fish dies and was fixed to 30 days according to shad ecology (Olney et al. 2006; Aunins and Olney 2009).

For iteroparous individuals that survive reproduction, nutrient imports are only a function of gamete inputs and excretion (Eq. 5)

(5) $$Is_{k,j}^n = \sum_{s \in \{male,\, female\}} Ns_{k,s,j} \times W_s \times \left(\eta_s^n + RT \times \tau^n\right)$$

Where $Ns_{k,s,j}$ is either the number of male and female spawners (both autochthonous and allochthonous) surviving reproduction in basin j, $W_{g,s}$ is the wet mass of testes or ovaries and $\eta_{g_s}^n$ is the nutrient content (% N and %P) of male or female gonads. The total wet mass of gamete inputs W_g was estimated as the difference between spawned and unspawned gonad masses, which were both modeled as a function of length (Table 1; Eq. 6 and 6'). As previously defined for carcass weight W, separate weight-length relationships were defined for each sex. For the unspawned gonad mass, both relationships were derived from fish captured during the 2008-2018 period at Golfech and Tuilières dams on the Garonne and Dordogne Rivers, respectively. The relationships for spawned gonad mass were derived from the same geographical location after artificial reproduction at the Bruch experimental station. Data were obtained from the non-profit association MIGADO (http://www.migado.fr/).

388

389 (6) $W_{g,m} = 13.9926 \times 10^{-5} \times L_m^{3.3838} - 1.2560 \times 10^{-5} \times L_m^{3.8331}$

390 (6') $W_{g,f} = 528.702 \times 10^{-5} \times L_f^{2.6729} - 132.890 \times 10^{-5} \times L_f^{2.8545}$

391

392 The percent wet mass content of N and P for eggs and sperm were approximated using values
393 for ovaries and testes taken from American shad, with $\eta_{g,m}^N$ = 0.0325 and $\eta_{g,m}^P$ =0.00724 for
394 males and $\eta_{g,f}^N$ = 0.03242 and $\eta_{g,f}^P$ =0.0032 for females (Haskell 2018) (Table 1).

395

396 3.2. Quantifying nutrient exports

397 The total export of nutrients conveyed by out-migrating juveniles from the river to the sea
398 was calculated as follows (Eq. 7):

399

400 (7) $E_j^n = No_j \times Wo_j \times \eta_o^n$

401

402 The offspring abundance No_j in basin *j* derived from GR3D was multiplied by the wet mass of
403 juvenile W_{o_j} and its nutrient content η_o^n (%N and %P). As was done for adults spawners, the
404 wet mass of juveniles was described as a function of juvenile length *L* and was based on the
405 relationship derived from Taverny (1991) (Table 1):

406

407 (8) $W_o = 6.9864 \times 10^{-3} \times L^{3.0306}$

408

409 The percent nutrient content of emigrating juveniles was provided by Haskell (2018) as η_o^N =
410 0.028 and η_j^P =0.00887.

411 Table 1: Inputs used in the nutrient routine for allis shad. The two parameters α and *b* were
412 derived from weight-length relationships. Data sources from which model inputs were derived
413 were indicated in the footnotes.

Measurements	Nominal values			
	α	*b*	%N (wet)[(b)]	%P (wet)[(b)]
Female				
W_T[(a)]	2.6654×10^{-3}	3.343	2.958	0.673
Pre-spawn ovary [(c)]	528.702×10^{-5}	2.673	3.242	0.320
Post-spawn ovary [(c)]	132.890×10^{-5}	2.854		
Male				
W_T[(a)]	4.0958×10^{-3}	3.225	2.941	0.666
Pre-spawn teste [(c)]	13.9926×10^{-5}	3.384	3.250	0.724
Post-spawn teste [(b)]	1.2560×10^{-5}	3.833		
Juveniles				
W_{Tj} [(a)]	6.9864×10^{-3}	3.031	2.803	0.887

414 [(a)]Taverny (1991), [(b)] Haskell (2018), [(c)] Computed from data provided by MIGADO

415

416 3.3. Quantifying nutrient interdependencies between river basins

417 Nutrient inputs supported by the population dynamics of spawners across the 135 river
418 basins were computed based on the natal origin of individuals (i.e donor basins, where fish
419 were born) and the destination where fish are showing up to spawn (i.e. recipient basins,
420 where spawner migrate to reproduce). When the natal basin was also the destination basin,
421 fish were considered 'autochthonous'. On the other hand, when the natal and destination
422 basins were different, fish were labelled as 'allochthonous'. Autochthonous fish were homers,
423 i.e. fish coming back to their natal river basin to reproduce, while allochthonous fish were
424 strayers wandering from other river basins. So, for each destination basin *j,* the import of N
425 and P was computed as the inputs provided by autochthonous fish that either die or survive
426 after reproduction ($Id^n_{j,\,auto,}\, Is^n_{j,\,auto}$) and those related to allochthonous fish ($Id^n_{j,\,allo,}$
427 $Is^n_{j,\,allo,\,,}$).

428 The relative nutrient contribution between autochthonous and allochthonous fish was
429 related to the species dispersal dynamics. For this modeling attempt, we considered the same
430 homing fidelity for all the rivers, so that 75% of fish returned to the natal river to spawn (P_{hom}

set to the high value of 0.75, see Table A1 and Rougier et al. (2014) for more details). For strayers, the probability of migrating to a destination basin increased as the distance between natal and destination basins decreased. Therefore, it was more likely for a fish to spawn in neighboring basins than basins located far away from the natal river, as explained in 1.1.

For each destination basin, the annual input of N and P was averaged over the period 1900-1930 to provide an average estimate of the 'maximal potential' for fish to deliver nutrients over this period (Eq. 9):

$$(9)\quad \overline{I_j^n} = \frac{1}{31} \times \sum_{t=1900}^{1930} Id_{j,auto}^n(t) + Is_{j,auto}^n(t) + Id_{j,allo}^n(t) + Is_{j,allo}^n(t)$$

The nutrient inputs supported by allochthonous fish (i.e. strayers) over the 135 river basins were represented with a Chord Diagram using the R-package 'Circlize' (Gu 2014; https://CRAN.R-project.org/package=circlize) widely used in population dynamics and genetics to quantify human migrations or gene flows. River basins were displayed all around a circle and connected with links corresponding to nutrient subsidies related to allochthonous fish. An in-depth analysis of the nutrient dynamics at the river-basin scale was performed using the Garonne River as a case study because the Garonne River was the reference population for shad in Europe and, as such, was carefully studied by the scientific community. Nutrient subsidies moving in and out of the Garonne River basin were represented with a Sankey diagram using the R package 'networkD3' (Allaire et al. 2017; https://CRAN.R-project.org/package=networkD3). Similar to the range-scale analysis, this method allows displaying the amount of nutrients supplied by fish migrating from one river to another with arrows indicating the magnitude of these inputs.

454 **Results**

455 1. Partial validation of abundance estimates

456 For the 13 river basins used to assess the global accuracy of model outputs, estimates of
457 abundance provided by the GR3D model were higher than the observed values in almost all
458 river basins (85%) except for the Vire and the Orne Rivers in France (Table 2). Nonetheless,
459 the differences in order of magnitude between observations and simulations were highly
460 variable across river basins, reflecting, to some extent, the variety of observational data used
461 for comparison through the study area. Almost half of the 13 river basins (48%) were
462 classified in Category 4, for which model outputs were much higher (i.e. above ten times
463 higher) than the observations and the majority of the remaining river basins (38%) were
464 placed into intermediate categories 2 and 3, for which models outputs and observations were
465 of the same order of magnitude.

466

467 Table 2: Comparison between GR3D estimated abundances and observed data for 13 river
468 basins along the European Atlantic coast. Seasonal model outputs and observations were
469 averaged over the same time period, with minimum and maximum values provided. River
470 basins were ordered by latitude from Portugal to France. A quality code ranging from
471 Category 1 to Category 4 was used to highlight the agreement between model estimates and
472 observed values. Category 1 indicated model outputs were lower than observed values and
473 thus judged as inaccurate. Categories 2, 3, and 4 indicated model outputs were higher than
474 observed values with increasing differences. The highest agreement was seen for intermediate
475 categories 2 and 3. Data sources are indicated in the footnotes.

476

477

478

River basin name (Country)	Year	Observations		GR3D outputs	Quality code
		Abundance (annual mean with minimum and maximum values in number of fish)	Data type	Abundance (annual mean with minimum and maximum values in number of fish)	
Lima (Portugal)	1990s	3 000 [1 000 – 5 000]	Fisheries[(a)]	57 851 [50 036 – 66 328]	4
Minho (Spain)	1914 – 1944	78 400 [15 000 – 105 000]	Fisheries[(a,b)]	123 761 [100 979 – 163 581]	2
Nivelle (France)	1998 – 2008	300 [29 – 688]	Entrapement/ Video counting at fishways[(c)]	6 975 [6 105 – 8 048]	4
Adour (France)	1985 – 1999	11 176 [NA]	Professional fisheries [(a,d)]	86 961 [66 131 – 112 105]	3
Garonne (France)	1996 – 2006	94 392 [46 409 – 161 306]	Video counting at Golfech and splash-based estimations [(c)]	446 096 [369 249 – 497 017]	3
Charente (France)	2010- – 2016*	26 046 [16 893 – 38 502]	Splash-based estimations [(f)]	106 831 [90 080 – 134 357]	3
Loire (France)	1998 – 2008	10 320 [1 200 – 31 418]	Video counting at fishways[(e)]	669 405 [555 001 – 781 317]	4
Vilaine (France)	1996 – 2006	918 [54 – 2,618]	Video counting at Arzal [(c,g)]	103 951 [92 436 – 118 848]	4
Scorff (France)	1996 – 2006	39 [2 – 188]	Entrapement/ Video counting at Moulin des Princes [(g)]	28 501 [24 810 – 33 057]	4
Aulne (France)	2000 – 2010	3 353 [399 – 6 714]	Video counting at Chateaulin [(c,g)]	8 967 [7 229 – 10 005]	3

Elorn (France)	2007 – 2010	380 [202 – 508]	Video counting at Kerhamon (*c,g*)	4 464 [4 273 – 4 735]	4
Vire (France)	2002 – 2010	4 258 [1 751 – 8 000]	Video counting at Claies de Vire (*c,g*)	198 [109 – 276]	1
Orne (France)	2002 – 2010	201 [50 – 406]	Video counting at Feuguerolles (*c,g*)	51 [28 – 74]	1

*GR3D estimates were provided for the 1996 – 2006 period as there is no temperature available after 2010 in the CRU database.

(*a*) ICES (2015), (*b*) Mota (2014), (*c*) P.Jatteau (personal observations, 2015), (*d*) Baglinière and Elie (2001), (*e*) Logrami (http://www.logrami.fr/), (*f*) EPTB Charente (https://www.fleuve-charente.net/), (g) Plagepomi https://www.observatoire-poissons-migrateurs-bretagne.fr/

2. Nutrient dynamics in the Garonne river basin case study

Over the 1900-1930 period, allis shad conveyed an average load of 0.324 (± 0.048) $kgN.km^2.year^{-1}$ and 0.055 (±0.008) $kgP.km^2.year^{-1}$ in the Garonne river basin. Shad were net importers of N and P, as the total amount of nutrient subsidies brought by spawners was higher than nutrients exported by out-migrating juveniles ($0.003 \pm 7.862 \times 10^{-4}$ $kgN.km^2.year^{-1}$ and $9.621 \times 10^{-4} \pm 2.488 \times 10^{-4}$ respectively). Regarding the source-sinks dynamics, most shad-derived nutrients were imported by autochthonous fish (97.1% of the total nutrient imports) and, to a lesser extent, by fish originating from neighboring river basins such as the Dordogne (1.91%), Charente (0.47%), and Loire (0.21%) rivers (Figure 2). The other donor river basins contributed less than 0.1% each to the amount of nutrients imported in the Garonne over 1900-1930. The Garonne river basin produced more strayers than it received. Most of the strayers from the Garonne river basin migrated to the Charente, Seudre, Dordogne, Lay, Sèvre Niortaise, Auzance and Leyre river basins, all in France.

3. Nutrient flows at the Atlantic area scale

A noticeable variability in annual net budget (import minus export) was calculated across river basins for both nutrients, ranging from 8.10^{-6} $kgN.km^2.year^{-1}$ to 1.2×10^4 $kgN.km^2.year^{-1}$

and 1.4 x 10^{-6} kgP.km^2.year^{-1} to 2.1 x 10^3 kgP.km^2.year^{-1}. Most river basins received both allochthonous and autochthonous individuals. The contribution of autochthonous individuals to the total import was also highly variable, ranging from 2.09% in the Taff River (U.K.) to 99.23% in the Loire River (France) (Figure 3). The Chord Diagram distinguished between river basins that produced more strayers than they received ('source-like') and river basins that received more strayers than they produced ('sink-like') (Figure 4). River basins located at the southern edge of the distribution, such as the Guadalquivir, Guadiana, Tagus, and Douro rivers in the Iberian Peninsula, as well as the Loire and Garonne rivers in France, were identified as the main producers of strayers. On the contrary, the Piedras, Tinto, Odiel, and Sado rivers in Spain and Portugal appeared as the main destinations for stayers along the Atlantic Area.

Discussion

Strengths and limits of the methodology

By combining a nutrient routine with a mechanistic species distribution model, the capacity of shad to move N and P subsidies between marine and freshwater ecosystems across their distribution range was quantitatively assessed. This work constituted one of the first evaluations of the regulating services associated with a diadromous fish species across its distribution range. Compared to river basin-specific assessments, this study brought substantial insights into the interdependencies between river basins regarding nutrient supplies related to anadromous species.

As our model was calibrated on historical presences and absences, abundance estimates provided by the model required validation using observed data (Table 2). These results suggested a somewhat limited agreement between model outputs and existing data, with estimated abundances much higher than observations in half of the 13 river basins used for validation (i.e. Category 4). For rivers with monitoring data included both shad species, model overestimation would likely be higher by considering a relatively low number of allis shad. However, the model coherence would remain the same, according to the validation index used. One explanation for these large differences is that reliable monitoring of shad populations started at the end of the 20th century (after 1950), when significant declines in most spawning stocks had already occurred. The GR3D simulations did not integrate anthropogenic pressures, meaning that abundance estimates represented a 'maximum potential'. In addition, observations were mostly based on a single data source that cannot be representative of the overall fish stock. For abundance estimates derived from counting at fishways, the data reliability is depending on the location of the device. If fish mostly spawn downstream of the dam, fish may not cross the barriers and therefore would not be counted by the device. These points, in addition to any inherent biases in the monitoring data, indicated

that the comparison between observed and estimated abundances was only valid if the sign and magnitude of the differences were considered and not the absolute values. Using this criterion, the partial model validation indicated overall confidence in the abundance estimates in the central and southern parts of the species range. However, simulations using previous and current GR3D versions indicated that the model estimates are less reliable throughout the northern range of allis shad, underestimating fish abundances in northern France (the Vire and Orne rivers in Table 2) up to Germany (Rougier et al. 2014).

The nutrient balance in the Garonne river basin: a local analysis

Our model calculated that allis shad historically imported an average of 0.324 (± 0.048 $kgN.km^2.year^{-1}$) and 0.055 (±0.008 $kgP.km^2.year^{-1}$), in the Garonne river basin. These values are far below the total amounts of N and P loaded from external sources. For instance, the total nutrient export from the Garonne river basin into the coastal zone was estimated to be 5792 $t.month^{-1}$ for N and 224 $t.month^{-1}$ for P over the period 1991-1995 (Romero et al. 2013). These numbers for allis shad were also lower than the nitrogen and phosphorus loadings reported for other diadromous species. By comparison, Haskell (2018) found that the closely related American shad (*Alosa sapidissima*) imported over 15 000 kg N and 3 000 kg P annually in the John Day Reservoir (JDR) in the lower Columbia River over the 1997-2015 time period. Considering that the JDR has a surface area of 222.6 km^2, the total amount of nitrogen and phosphorus associated with American shad spawning runs would be 67.38 $kg.N.km^2.year^{-1}$ and 13.48 $kgP.km^2.year^{-1}$. However, these estimates were for a specific reservoir within the Columbia River watershed, while the nutrients subsidized by allis shad were for the entire Garonne watershed. To be consistent, nutrient estimates must be displayed at a similar scale. Considering water surface only covers 1% of the whole Garonne River

559 watershed (BD TOPAGE, https://bdtopage.eaufrance.fr/), the amount of N and P load by allis
560 shad population would be over 31.130 kgN.km^2.year^{-1} and 5.290 kgP.km^2.year^{-1}.
561 These values were still below those founded for the American shad in the JDR, but were
562 supported by a smaller population size (467 000 for almost 1 billion entering the JDR
563 (Haskell 2018).
564 The ecological meaning of these nutrient subsidies is a function of the baseline nutrient
565 levels of riverine waters. For oligotrophic rivers where nitrogen and phosphorus tend to be
566 limiting resources, even low levels of enrichment by migratory organisms such as shad would
567 be significant enough to increase the ecosystem productivity (Durbin et al. 1979). Although,
568 for the Garonne River, the significance of these nutrient subsidies should be examined by
569 considering the timing to which resources are delivered and where. Anadromous species
570 spawn seasonally in specific and restricted areas, so they provide a condensed pulse of
571 nutrients over a short period of time (Weber and Brown 2018). In rivers, the availability of N
572 and P to an aquatic organism varies according to its trophic status, the season, riverine inputs,
573 and biogeochemical and bacterial activity.
574 Along the European Atlantic coast, allis shad spawn in the spring when primary
575 productivity in rivers is starting to increase, and riverine inputs of N and P from upstream
576 reaches start to become relatively low due to decreasing river discharge. Under such
577 environmental conditions, carcasses were unlikely to be washed out or moved downstream
578 over substantial distances from the spawning grounds (Garman 1992). Hence, carcass
579 decomposition may provide a relatively steady source of nutrients for several weeks, and N
580 and P subsidies delivered in spring and summer may have a larger impact on ecosystem
581 functioning than suggested by the total annual amounts alone.
582 This study provided the first quantification of nutrient fluxes transported by allis shad
583 from marine to freshwater ecosystems at the distribution range scale, but it did not investigate

584 the trophic pathways of marine-derived nutrients incorporation into riverine food webs.
585 Previous studies have explored the contribution of fish-derived nutrients into riverine and
586 lacustrine food webs using stable isotope analyses (Kohler et al. 2012; Guyette et al. 2014;
587 Samways et al. 2018). Marine-derived nutrients enter food webs either through direct
588 consumption of marine-derived organic matter (e.g. carcasses or eggs) by predators and
589 scavengers or through indirect uptake of dissolved nutrients by bacteria and other autotrophic
590 organisms (Samways et al. 2018). For several anadromous species, both pathways were
591 suggested as a primary source of nutrients, depending on the location of populations. In a
592 small Alaskan system, Gende et al. (2004) demonstrated that almost 50% of the salmons
593 derived-nutrients in the stream was directly incorporated into the riverine food web through
594 predation by bears. Like salmons, alewives may also subsidize higher trophic levels directly
595 as a food resource for a wide variety of aquatic predators (Flecker et al. 2010) or may be
596 incorporated via the bottom-up trophic pathways. For instance, Walters et al. (2009) showed
597 that the indirect uptake by periphyton of dissolved nutrients released from excretion and
598 carcass decomposition was then delivered to higher trophic levels such as macro-
599 invertebrates.

600 So far, the contribution of allis shad to riverine food webs remains unexplored. Given the
601 species' semelparous existence, with most fish dying after reproduction, allis shad-derived
602 nutrients would be first incorporated through direct consumption of carcasses by
603 macroinvertebrates (Fenoglio et al. 2010). In the Rappahannock River system (Virginia),
604 MacAvoy et al. (2000) did not find evidence of shad-derived marine nutrients at lower trophic
605 levels, suggesting that shad would have a greater influence acting as prey for carnivorous fish
606 and birds (Garman and Macko 1998; MacAvoy et al. 2000; Haskell 2018).

607

608 *Diadromous species as valuable cross-border resources*

609 By examining the nutrient dynamics related to shad throughout its entire distribution
610 range, this study mapped the main locations of nutrient provision and destination across the
611 European coast of the Atlantic Ocean. Most river basins in GR3D received substantial N and
612 P subsidies imported by strayers from the marine system, suggesting that each river basin
613 supports the provision of ecosystem services in other locations but some more than others.
614 Since the straying rate was the same for all the river basins considered, these differences were
615 mainly driven by the size of the catchment. Large catchments produced more spawners and
616 thus more individuals that would stray to nearby rivers. Similarly, depending on the location
617 of the rivers along the Atlantic arc, the size, and the number of neighboring basins,
618 contributions of autochthonous or allochthonous species are expected to change accordingly.
619 These findings are partly corroborated by the study conducted by Randon et al. (2018).
620 Using otolith microchemistry and a Bayesian approach, these authors identified major
621 'source' and 'sink' subpopulations across 18 rivers sampled in France and Portugal. Results
622 suggested that multiple exchanges occurred among rivers, contrasting with the high level of
623 homing presumed for this species (Jolly et al. 2012; Martin et al. 2015). In their study, the
624 Dordogne and Minho rivers appeared to be 'sources', defined as a river 'which produced
625 more individuals than received', while the Loire, Garonne, and Mondego rivers received a
626 high percent of strayers compared to homers. The Garonne river basin appeared as a main
627 'sink' with 99.9% of fish being strayers from neighboring rivers. Conversely, the present
628 modeling results revealed that 98% of N and P inputs in the Garonne river basin were
629 historically provided by homers. Nonetheless, in the current study, most of the allochthonous
630 spawners coming to the Garonne river basin were, in fact, born in the Dordogne river basin, as
631 was seen in the study of Randon et al. (2018). In addition, some of the largest river basins
632 such as the Douro and Tagus in Portugal, known as important allis shad populations, were not
633 considered by Randon et al. (2018), forcing the reallocation by the Bayesian model of adults

634 into other chemically similar rivers and limiting the interpretation of exchanges based on
635 microchemistry analyses.

636 These two studies put together confirmed that conservation efforts in the Gironde-
637 Garonne-Dordogne system would benefit from the recognition of linkages between these two
638 river basins even if the intensity of this relationship is still to be determined. More broadly,
639 the amount of nutrient flow sustained by the metapopulation dynamics of spawners in the
640 present study argues for cross-border cooperative management efforts instead of catchment-
641 specific measures (www.diades.eu).

642

643 *Implications for management in a globally changing environment*

644 The management of migratory species is a complex issue as it raises questions on the
645 scale necessary for such operations (Runge et al. 2014). As seen in the present results, the
646 significant exchanges of individuals between river basins, delivering and receiving nutrient
647 subsidies from fish produced at various locations, confirmed the need to shift from local (river
648 basin-specific) to cross-jurisdictional and cross-border cooperative strategies for managing
649 allis shad populations (Semmens et al. 2011; www.diades.eu). This change of perspective is
650 especially urgent when considering the shifts in distribution observed and predicted for many
651 animal and plant species under climate change, including diadromous species impacted by
652 changes in temperature and precipitation patterns (Parmesan and Yohe 2003; Lassalle and
653 Rochard 2009). The situation is obviously changing, causing new socio-economic and
654 ecological interactions among territories that might increase the spatial mismatches between
655 areas where services are produced and consumed (Semmens et al. 2011).

656 This study provided estimates of the maximum capacity of shad to convey nutrients
657 across the landscape. However, despite abundant shad stocks calculated by the model in the
658 early 20th century with no anthropogenic pressures at play, the level of nutrients delivered by

659 'pristine' populations seemed low compared to those estimated for other related species and
660 from other sources (e.g. atmospheric deposition, fertilizers, and wastewater). However, one
661 should consider the timing of such inputs (i.e. spring/summer) and the concentration of fish at
662 specific places (i.e. spawning grounds) before concluding that allis shad provide a negligible
663 nutrient subsidy. Considering the massive decline of spawning populations that occurred over
664 the last century and the projected reduction in fish body size (Daufresne et al. 2009), nutrient
665 inputs could be even more reduced by the end of the century (Twining et al. 2017).

Author statements

Acknowledgements:

This study was co-funded by Agence de l'Eau Adour Garonne and Nouvelle Aquitaine Region within the SHAD'EAU/FAUNA projects (coordination: Françoise Daverat (INRAE)) and the Atlantic Area Interreg Project DiadES (coordination: Géraldine Lassalle (INRAE) and Patrick Lambert (INRAE)). Many thanks go to the Fundación para la Investigación del Clima (FIC; https://www.ficlima.org/) for providing the CRU database temperature extraction. We are grateful to the French non-profit association MIGADO (http://www.migado.fr/) for giving us access to shad biological characteristics at the Bruch experimental station. We also wanted to thank Sébastien Boutry (INRAE) for his sound advices in data visualization technics and the two anonymous reviewers for their constructive remarks on the manuscript.

Contributors'statement: All authors contributed to the study conceptualization and writing. A first draft was written by CP, and then all authors commented on previous versions of the manuscript. All authors read and approved the final manuscript. CP and PL contributed to the software development.

Funding statement: This research was co-funded by Agence de l'Eau Adour Garonne and Nouvelle Aquitaine Region within the SHAD'EAU/FAUNA projects (coordination: Françoise Daverat (INRAE)) and the Atlantic Area Interreg Project DiadES (coordination: Géraldine Lassalle (INRAE) and Patrick Lambert (INRAE)).

Data availability statement: The updated GR3D code can be openly accessed at http://doi.org/10.5281/zenodo.4442030 or directly following the URL https://github.com/inrae/GR3D/tree/v3.2.1.

References

Allaire, J.J., Gandrud C., Russell K and Yetman, CJ. 2017. NetworkD3: D3 JavaScript Network Graphs from R. R package version 0.4. https://CRAN.R-project.org/package=networkD3

Auer, S.K., Anderson, G.J., McKelvey, S., Bassar, R.D., McLennan, D., Armstrong, J.D., Nislow, K.H., Downie, H.K., McKelvey, L., Morgan, T.A.J., Salin, K., Orrell, D.L., Gauthey, A., Reid, T.C., and Metcalfe, N.B. 2018. Nutrients from salmon parents alter selection pressures on their offspring. Ecol Lett **21**(2): 287–295. doi:10.1111/ele.12894.

Aunins, A., and Olney, J.E. 2009. Migration and Spawning of American Shad in the James River, Virginia - Aunins - 2009 - Transactions of the American Fisheries Society - Wiley Online Library.

Baglinière, J.-L., and Élie, P. 2000. Les aloses, Alosa alosa et Alosa fallax spp.: écobiologie et variabilité des populations. Institut national de la recherche agronomique, Paris.

Bal, G., Rivot, E., Prévost, E., Piou, C., and Baglinière, J.L. 2011. Effect of water temperature and density of juvenile salmonids on growth of young-of-the-year Atlantic salmon Salmo salar. Journal of Fish Biology **78**(4): 1002–1022. doi:https://doi.org/10.1111/j.1095-8649.2011.02902.x.

Barber, B.L., Gibson, A.J., O'Malley, A.J., and Zydlewski, J. 2018. Does What Goes up Also Come Down? Using a Recruitment Model to Balance Alewife Nutrient Import and Export. Marine and Coastal Fisheries **10**(2): 236–254. doi:10.1002/mcf2.10021.

Beverton, R.J.H., and Holt, S.J. 1957. On the dynamics of exploited fish populations. London : H.M. Stationery Off.

Bilby, R.E., Fransen, B.R., and Bisson, P.A. 1996. Incorporation of nitrogen and carbon from spawning coho salmon into the trophic system of small streams: evidence from stable

isotopes. Canadian Journal of Fisheries and Aquatic Sciences. NRC Research Press Ottawa, Canada. doi:10.1139/f95-159.

Bolster, W.J. 2008. Putting the Ocean in Atlantic History: Maritime Communities and Marine Ecology in the Northwest Atlantic, 1500–1800. The American Historical Review **113**(1): 19–47. doi:10.1086/ahr.113.1.19.

Castelnaud, G., Rochard, E., and Le Gat, Y. 2001. Analyse de la tendance de l'abondance de l'alose alosa alosa en gironde à partir de l'estimation d'indicateurs halieutiques sur la période 1977-1998. Bulletin Français de la Pêche et de la Pisciculture (362–363): 989–1015. doi:10.1051/kmae:2001032.

Daufresne, M., Lengfellner, K., and Sommer, U. 2009. Global warming benefits the small in aquatic ecosystems. PNAS **106**(31): 12788–12793.

Drouineau, H., Carter, C., Rambonilaza, M., Beaufaron, G., Bouleau, G., Gassiat, A., Lambert, P., le Floch, S., Tétard, S., and de Oliveira, E. 2018. River Continuity Restoration and Diadromous Fishes: Much More than an Ecological Issue. Environmental Management **61**(4): 671–686. doi:10.1007/s00267-017-0992-3.

Dumoulin, N. 2007. SimAquaLife : un cadriciel pour la modélisation de la dynamique spatiale d'organismes aquatiques. Techniques et sciences informatiques **26**(6): 701–721. doi:10.3166/tsi.26.701-721.

Durbin, A.G., Nixon, S.W., and Oviatt, C.A. 1979. Effects of the Spawning Migration of the Alewife, Alosa Pseudoharengus, on Freshwater Ecosystems. Ecology **60**(1): 8–17. doi:10.2307/1936461.

Fenoglio, S., Bo, T., Cammarata, M., Malacarne, G., and Del Frate, G. 2010. Contribution of macro- and micro-consumers to the decomposition of fish carcasses in low-order streams: an experimental study. Hydrobiologia. Dordrecht : Springer Netherlands.

Flecker, A., McIntyre, P.B., Moore, J.W., Anderson, J., Taylor, B., and Hall, R. 2010. Migratory fishes as material and process subsidies in riverine ecosystems. American Fisheries Society Symposium **73**: 559–592.

Garibaldi, A., and Turner, N. 2004. Cultural Keystone Species: Implications for Ecological Conservation and Restoration. Ecology and Society **9**. doi:10.5751/ES-00669-090301.

Garman, G.C. 1992. Fate and Potential Significance of Postspawning Anadromous Fish Carcasses in an Atlantic Coastal River. null **121**(3): 390–394. Taylor & Francis. doi:10.1577/1548-8659(1992)121<0390:FAPSOP>2.3.CO;2.

Garman, G.C., and Macko, S.A. 1998. Contribution of Marine-Derived Organic Matter to an Atlantic Coast, Freshwater, Tidal Stream by Anadromous Clupeid Fishes. Journal of the North American Benthological Society **17**(3): 277–285. doi:10.2307/1468331.

Gende, S.M., Quinn, T.P., Willson, M.F., Heintz, R., and Scott, T.M. 2004. Magnitude and Fate of Salmon-Derived Nutrients and Energy in a Coastal Stream Ecosystem. Journal of Freshwater Ecology **19**(1): 149–160. Taylor & Francis. doi:10.1080/02705060.2004.9664522.

Gilligan-Lunda, E.K., Stich, D.S., Mills, K.E., Bailey, M.M., and Zydlewski, J.D. 2021. Climate Change May Cause Shifts in Growth and Instantaneous Natural Mortality of American Shad Throughout Their Native Range. Trans Am Fish Soc **150**(3): 407–421. doi:10.1002/tafs.10299.

Gresh, T., Lichatowich, J., and Schoonmaker, P. 2000. An Estimation of Historic and Current Levels of Salmon Production in the Northeast Pacific Ecosystem: Evidence of a Nutrient Deficit in the Freshwater Systems of the Pacific Northwest. Fisheries **25**(1): 15–21. doi:10.1577/1548-8446(2000)025<0015:AEOHAC>2.0.CO;2.

Gu, Z., Gu, L., Eils, R., Schlesner, M., Brors, B. 2014. Circlize implements and enhances circular visualization in R. Bioinformatics, 30, 2811-2812. https://CRAN.R-project.org/package=circlize

Guyette, M.Q., Loftin, C.S., Zydlewski, J., and Cunjak, R. 2014. Carcass analogues provide marine subsidies for macroinvertebrates and juvenile Atlantic salmon in temperate oligotrophic streams. Freshwater Biology **59**(2): 392–406. doi:10.1111/fwb.12272.

Haro, A. 2009. Challenges for diadromous fishes in a dynamic global environment. American Fisheries Society.

Haskell, C.A. 2018. From salmon to shad: Shifting sources of marine-derived nutrients in the Columbia River Basin. Ecology of Freshwater Fish **27**(1): 310–322. doi:10.1111/eff.12348.

Hicks, C.C., Cohen, P.J., Graham, N.A.J., Nash, K.L., Allison, E.H., D'Lima, C., Mills, D.J., Roscher, M., Thilsted, S.H., Thorne-Lyman, A.L., and MacNeil, M.A. 2019. Harnessing global fisheries to tackle micronutrient deficiencies. Nature **574**(7776): 95–98. doi:10.1038/s41586-019-1592-6.

Hyder, K., Weltersbach, M.S., Armstrong, M., Ferter, K., Townhill, B., Ahvonen, A., Arlinghaus, R., Baikov, A., Bellanger, M., Birzaks, J., Borch, T., Cambie, G., de Graaf, M., Diogo, H.M.C., Dziemian, Ł., Gordoa, A., Grzebielec, R., Hartill, B., Kagervall, A., Kapiris, K., Karlsson, M., Kleiven, A.R., Lejk, A.M., Levrel, H., Lovell, S., Lyle, J., Moilanen, P., Monkman, G., Morales-Nin, B., Mugerza, E., Martinez, R., O'Reilly, P., Olesen, H.J., Papadopoulos, A., Pita, P., Radford, Z., Radtke, K., Roche, W., Rocklin, D., Ruiz, J., Scougal, C., Silvestri, R., Skov, C., Steinback, S., Sundelöf, A., Svagzdys, A., Turnbull, D., van der Hammen, T., van Voorhees, D., van Winsen, F., Verleye, T., Veiga, P., Vølstad, J.-H., Zarauz, L., Zolubas, T., and Strehlow, H.V. 2018. Recreational sea fishing in Europe in a global

context-Participation rates, fishing effort, expenditure, and implications for monitoring and assessment. Fish and Fisheries **19**(2): 225–243. doi:10.1111/faf.12251.

ICES 2015. Report of the Workshop on Lampreys and Shads (WKLS), 27-29 November 2014, Lisbon, Portugal. ICES CM 2014/SSGEF:13. 206 pp.

IUCN 2020. The IUCN Red List of Threatened Species. Version 2020-3. https://www.iucnredlist.org.

Janetski, D.J., Chaloner, D.T., Tiegs, S.D., and Lamberti, G.A. 2009. Pacific salmon effects on stream ecosystems: a quantitative synthesis. Oecologia **159**(3): 583–595. doi:10.1007/s00442-008-1249-x.

Jatteau, P., Drouineau, H., Charles, K., Carry, L., Lange, F., and Lambert, P. 2017. Thermal tolerance of allis shad (*Alosa alosa*) embryos and larvae: Modeling and potential applications. Aquatic Living Resources **30**: 2. doi:10.1051/alr/2016033.

Jolly, M.T., Aprahamian, M.W., Hawkins, S.J., Henderson, P.A., Hillman, R., O'Maoiléidigh, N., Maitland, P.S., Piper, R., and Genner, M.J. 2012. Population genetic structure of protected allis shad (Alosa alosa) and twaite shad (Alosa fallax). Mar Biol **159**(3): 675–687. doi:10.1007/s00227-011-1845-x.

Joordens, J.C.A., Kuipers, R.S., Wanink, J.H., and Muskiet, F.A.J. 2014. A fish is not a fish: Patterns in fatty acid composition of aquatic food may have had implications for hominin evolution. Journal of Human Evolution **77**: 107–116. doi:10.1016/j.jhevol.2014.04.004.

Kielbassa, J., Delignette-Muller, M.L., Pont, D., and Charles, S. 2010. Application of a temperature-dependent von Bertalanffy growth model to bullhead (Cottus gobio). Ecological Modelling **221**(20): 2475–2481. doi:10.1016/j.ecolmodel.2010.07.001.

Kobayashi, M., Msangi, S., Batka, M., Vannuccini, S., Dey, M.M., and Anderson, J.L. 2015. Fish to 2030: The Role and Opportunity for Aquaculture. Aquaculture Economics & Management **19**(3): 282–300. doi:10.1080/13657305.2015.994240.

Kohler, A.E., Pearsons, T.N., Zendt, J.S., Mesa, M.G., Johnson, C.L., and Connolly, P.J. 2012. Nutrient Enrichment with Salmon Carcass Analogs in the Columbia River Basin, USA: A Stream Food Web Analysis. Transactions of the American Fisheries Society **141**(3): 802–824. doi:10.1080/00028487.2012.676380.

Kremen, C., Williams, N.M., Aizen, M.A., Gemmill-Herren, B., LeBuhn, G., Minckley, R., Packer, L., Potts, S.G., Roulston, T., Steffan-Dewenter, I., Vázquez, D.P., Winfree, R., Adams, L., Crone, E.E., Greenleaf, S.S., Keitt, T.H., Klein, A.-M., Regetz, J., and Ricketts, T.H. 2007. Pollination and other ecosystem services produced by mobile organisms: a conceptual framework for the effects of land-use change. Ecology Letters **10**(4): 299–314. doi:https://doi.org/10.1111/j.1461-0248.2007.01018.x.

Lassalle, G., and Rochard, E. 2009. Impact of twenty-first century climate change on diadromous fish spread over Europe, North Africa and the Middle East. Global Change Biology **15**(5): 1072–1089. doi:10.1111/j.1365-2486.2008.01794.x.

Limburg, K.E., and Waldman, J.R. 2009. Dramatic Declines in North Atlantic Diadromous Fishes. BioScience **59**(11): 955–965. doi:10.1525/bio.2009.59.11.7.

López-Hoffman, L., Varady, R.G., Flessa, K.W., and Balvanera, P. 2010. Ecosystem services across borders: a framework for transboundary conservation policy. Frontiers in Ecology and the Environment **8**(2): 84–91. doi:10.1890/070216.

MacAvoy, S.E., Macko, S.A., McIninch, S.P., and Garman, G.C. 2000. Marine nutrient contributions to freshwater apex predators. Oecologia **122**(4): 0568. doi:10.1007/s004420050980.

Martin, J., Rougemont, Q., Drouineau, H., Launey, S., Jatteau, P., Bareille, G., Berail, S., Pécheyran, C., Feunteun, E., Roques, S., Clavé, D., Nachón, D.J., Antunes, C., Mota, M., Réveillac, E., and Daverat, F. 2015. Dispersal capacities of anadromous Allis shad population inferred from a coupled genetic and otolith approach. Canadian Journal of Fisheries and Aquatic Sciences **72**(7): 991–1003. doi:10.1139/cjfas-2014-0510.

McDowall, R.M. 1988. Diadromy in fishes: migrations between freshwater and marine environments. Croom Helm.

Mennesson-Boisneau, C. 1990. Migration, répartition, reproduction et caractéristiques biologiques des aloses (Alosa sp.) dans le bassin de la Loire.

Mennesson-Boisneau, C., Aprahamian, M.W., Sabatié, M.R., and Cassou-Leins, J.J. 2000. Biologie des aloses : remontée migratoire des adultes. *In* Les aloses (*Alosa alosa* et *Alosa fallax spp.*) : écobiologie et variabilité des populations. *Edited by* J.L. Baglinière and P. Elie. Cemagref, Inra Éditions, Paris. pp. 55–72.

Millennium Ecosystem Assessment, 2005. Ecosystems and human well-being: synthesis. Island Press, Washington, DC.

Mota, M., Rochard, E., and Antunes, C. 2016. Status of the Diadromous Fish of the Iberian Peninsula: Past, Present and Trends. Limnetica (35): 1–18. doi:10.23818/limn.35.01.

Naiman, R.J., Bilby, R.E., Schindler, D.E., and Helfield, J.M. 2002. Pacific Salmon, Nutrients, and the Dynamics of Freshwater and Riparian Ecosystems. Ecosystems **5**(4): 399–417. doi:10.1007/s10021-001-0083-3.

Olney, J.E., Latour, R.J., Watkins, B.E., and Clarke, D.G. 2006. Migratory Behavior of American Shad in the York River, Virginia, with Implications for Estimating In-River Exploitation from Tag Recovery Data. Transactions of the American Fisheries Society **135**(4): 889–896. doi:10.1577/T05-101.1.

Parmesan, C., and Yohe, G. 2003. A globally coherent fingerprint of climate change impacts across natural systems. Nature **421**: 37.

Paumier, A., Drouineau, H., Carry, L., Nachón, D.J., and Lambert, P. 2019. A field-based definition of the thermal preference during spawning for allis shad populations (Alosa alosa). Environ Biol Fish **102**(6): 845–855. doi:10.1007/s10641-019-00874-7.

Post, D.M., and Walters, A.W. 2009. Nutrient Excretion Rates of Anadromous Alewives during Their Spawning Migration. Transactions of the American Fisheries Society **138**(2): 264–268. doi:10.1577/T08-111.1.

Randon, M., Daverat, F., Bareille, G., Jatteau, P., Martin, J., Pecheyran, C., and Drouineau, H. 2018. Quantifying exchanges of Allis shads between river catchments by combining otolith microchemistry and abundance indices in a Bayesian model. ICES Journal of Marine Science **75**(1): 9–21. doi:10.1093/icesjms/fsx148.

R Core Team (2018) R: A language and environment for statistical computing. R Foundation for Statistical Computing, Vienna, Austria.

Romero, E., Garnier, J., Lassaletta, L., Billen, G., Le Gendre, R., Riou, P., and Cugier, P. 2013. Large-scale patterns of river inputs in southwestern Europe: seasonal and interannual variations and potential eutrophication effects at the coastal zone. Biogeochemistry **113**(1–3): 481–505. doi:10.1007/s10533-012-9778-0.

Rosso, L., Lobry, J.R., Bajard, S., and Flandrois, J.P. 1995. Convenient Model To Describe the Combined Effects of Temperature and pH on Microbial Growth. Appl. Environ. Microbiol. **61**(2): 610.

Rougier, T. 2014. Repositionnement des poissons migrateurs amphihalins européens dans un contexte de changement climatique : une approche exploratoire par modélisation dynamique mécaniste. Ph.D. thesis, University of Bordeaux.

Rougier, T., Drouineau, H., Dumoulin, N., Faure, T., Deffuant, G., Rochard, E., and Lambert, P. 2014. The GR3D model, a tool to explore the Global Repositioning Dynamics of Diadromous fish Distribution. Ecological Modelling **283**: 31–44. doi:10.1016/j.ecolmodel.2014.03.019.

Runge, C.A., Martin, T.G., Possingham, H.P., Willis, S.G., and Fuller, R.A. 2014. Conserving mobile species. Frontiers in Ecology and the Environment **12**(7): 395–402. doi:10.1890/130237.

Samways, K., and Cunjak, R.A. 2010. The importance of marine derived nutrients delivered to Atlantic rivers by four species of anadromous fishes.

Samways, K.M., Quiñones-Rivera, Z.J., Leavitt, P.R., and Cunjak, R.A. 2015. Spatiotemporal responses of algal, fungal, and bacterial biofilm communities in Atlantic rivers receiving marine-derived nutrient inputs. Freshwater Science **34**(3): 881–896. doi:10.1086/681723.

Samways, K.M., Soto, D.X., and Cunjak, R.A. 2018. Aquatic food-web dynamics following incorporation of nutrients derived from Atlantic anadromous fishes: nutrients from anadromous fishes. Journal of Fish Biology **92**(2): 399–419. doi:10.1111/jfb.13519.

Scheuerell, M.D., Levin, P.S., Zabel, R.W., Williams, J.G., and Sanderson, B.L. 2005. A new perspective on the importance of marine-derived nutrients to threatened stocks of Pacific salmon (Oncorhynchus spp.). Can. J. Fish. Aquat. Sci. **62**(5): 961–964. doi:10.1139/f05-113.

Schindler, D.E., Scheuerell, M.D., Moore, J.W., Gende, S.M., Francis, T.B., and Palen, W.J. 2003. Pacific salmon and the ecology of coastal ecosystems. Frontiers in Ecology and the Environment **1**(1): 31–37. doi:10.1890/1540-9295(2003)001[0031:PSATEO]2.0.CO;2.

Semmens, D.J., Diffendorfer, J.E., Bagstad, K.J., Wiederholt, R., Oberhauser, K., Ries, L., Semmens, B.X., Goldstein, J., Loomis, J., Thogmartin, W.E., Mattsson, B.J., and López-Hoffman, L. 2018. Quantifying ecosystem service flows at multiple scales across the range of a long-distance migratory species. Ecosystem Services **31**: 255–264. doi:10.1016/j.ecoser.2017.12.002.

Semmens, D.J., Diffendorfer, J.E., López-Hoffman, L., and Shapiro, C.D. 2011. Accounting for the ecosystem services of migratory species: Quantifying migration support and spatial subsidies. Ecological Economics **70**(12): 2236–2242. doi:10.1016/j.ecolecon.2011.07.002.

Steffen, W., Broadgate, W., Deutsch, L., Gaffney, O., and Ludwig, C. 2015. The trajectory of the Anthropocene: The Great Acceleration. The Anthropocene Review **2**(1): 81–98. doi:10.1177/2053019614564785.

Stephens, P.A., Sutherland, W.J., and Freckleton, R.P. 1999. What Is the Allee Effect? Oikos **87**(1): 185–190. [Nordic Society Oikos, Wiley]. doi:10.2307/3547011.

Taverny, C. 1991. Contribution à la connaissance de la dynamique des populations d'aloses : Alosa Alosa et Alosa Fallax dans le système fluvio-estuarien de la Gironde : pêche, biologie et écologie : étude particulière de la devalaison et de l'impact des activités humaines.

Twining, C.W., Palkovacs, E.P., Friedman, M.A., Hasselman, D.J., and Post, D.M. 2017. Nutrient loading by anadromous fishes: species-specific contributions and the effects of diversity. Canadian Journal of Fisheries and Aquatic Sciences **74**(4): 609–619. doi:10.1139/cjfas-2016-0136.

Von Bertalanffy, L. 1938. A quantitative theory of organic growth (inquiries on growth laws. II). Human Biology **10**(2): 181–213.

Walters, A.W., Barnes, R.T., and Post, D.M. 2009. Anadromous alewives (*Alosa pseudoharengus*) contribute marine-derived nutrients to coastal stream food webs. Canadian Journal of Fisheries and Aquatic Sciences **66**(3): 439–448. doi:10.1139/F09-008.

Weaver, D.M., Coghlan, S.M., and Zydlewski, J. 2018. Effects of sea lamprey substrate modification and carcass nutrients on macroinvertebrate assemblages in a small Atlantic coastal stream. Journal of Freshwater Ecology **33**(1): 19–30. doi:10.1080/02705060.2017.1417168.

Weber, M.J., and Brown, M.L. 2018. Effects of resource pulse magnitude on nutrient availability, productivity, stability, and food web dynamics in experimental aquatic ecosystems. Hydrobiologia **814**(1): 191–203. doi:10.1007/s10750-018-3536-9.

West, D.C., Walters, A.W., Gephard, S., and Post, D.M. 2010. Nutrient loading by anadromous alewife (Alosa pseudoharengus): contemporary patterns and predictions for restoration efforts. Canadian Journal of Fisheries and Aquatic Sciences **67**(8): 1211–1220. doi:10.1139/F10-059.

Wilson, K.; And Veneranta, L. (Eds.). 2019. Data-limited diadromous species ? review of European status. ICES. doi:10.17895/ICES.PUB.5253.

Wipfli, M.S., Hudson, J.P., Caouette, J.P., and Chaloner, D.T. 2003. Marine Subsidies in Freshwater Ecosystems: Salmon Carcasses Increase the Growth Rates of Stream-Resident Salmonids. Transactions of the American Fisheries Society **132**(2): 371–381. doi:https://doi.org/10.1577/1548-8659(2003)132<0371:MSIFES>2.0.CO;2.

Figure captions

Figure 1. Structure of the GR3D model after integration of the new nutrient routine. In the ocean, mature fish disperse in freshwater to spawn. The number of recruits produced is determined by a Beverton-Holt spawners-recruits curve (BH-SR). The nutrient balance is based on adult import derived from dead (Id_j^n) or living fish (Is_j^n) and out-migrating juvenile export. See Appendix 1 for a fully detailed description with model equations.

Figure 2. Sankey diagram of the nitrogen flows associated with the Garonne river basin. All the river basins listed on the left were 'natal basins' and all the river basins on the right were 'destination basins'. The light grey band represented fish originating from the Garonne river basin and returning to the Garonne river basin (autochthonous fish). The four lines at the bottom indicated the origins of the allochthonous fish entering the Garonne river basin. Lines above the light grey band indicated the destinations of Garonne strayers in the Atlantic area. Lines were proportional to the net nitrogen import. River basins on the right were ordered by latitude, with the exception of the Garonne river basin.

Figure 3. Contribution of the autochthonous fish (in %) to the total import of nitrogen over the period 1900-1930 in the river basins colonized by shads in the GR3D physical environment. The remaining percent was for inputs derived from strayers coming from other rivers. River basins were ordered along a latitudinal gradient from Morocco to Germany.

Figure 4. Interdependencies among river basins in nitrogen supplies provided by allis shad allochthonous fish straying from one to another river (KgN) over the period 1900-1930. Each intermediate tick mark increases by 800 kgN, starting from 0. River basins were ordered

clockwise along a latitudinal gradient, ranging from the Oum Er-Rbia river basin at the southern edge of the distribution in Morocco (red) to the Avon river basin at the northern edge of the distribution in the U.K (blue). To ease the reading, only the nitrogen supplies provided by allochthonous fish contributing more than 10% of the total nutrient subsidies imported in each river basin were represented in the figure. The magnitude and flow of each relationship were indicated by arrow size and direction, respectively. A latitudinal color gradient was used to distinguish among arrows from different basins. The contribution of autochthonous fish was not represented in the Chord Diagram.

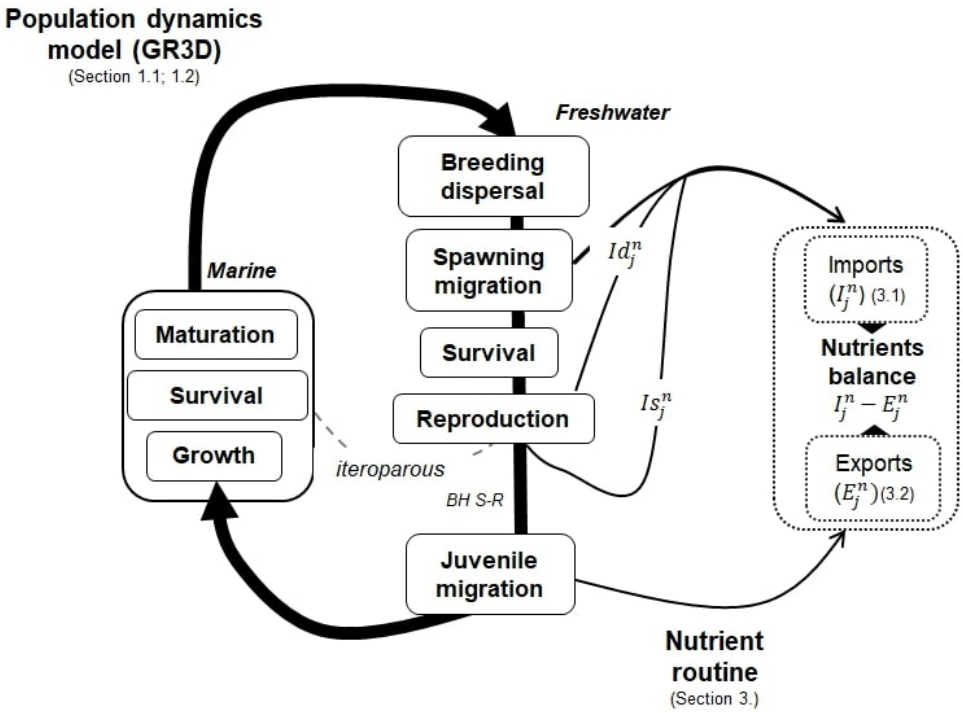

Figure 1. Structure of the GR3D model after integration of the new nutrient routine. In the ocean, mature fish disperse in freshwater to spawn. The number of recruits produced is determined by a Beverton-Holt spawners-recruits curve (BH-SR). The nutrient balance is based on adult import derived from dead (Id^n_j) or living fish (Is^n_j) and out-migrating juvenile export. See Appendix 1 for a fully detailed description with model equations.

271x201mm (72 x 72 DPI)

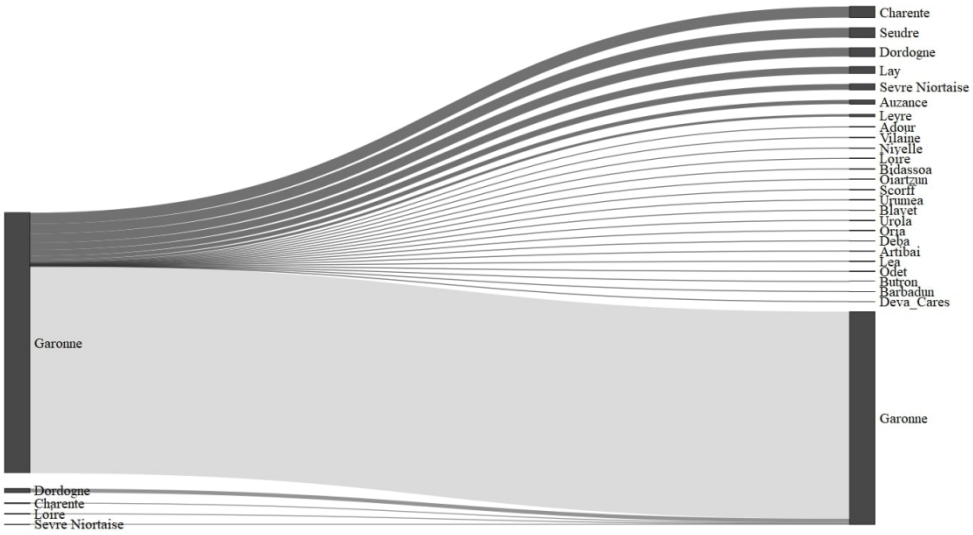

Figure 2. Sankey diagram of the nitrogen flows associated with the Garonne river basin. All the river basins listed on the left were 'natal basins' and all the river basins on the right were 'destination basins'. The light grey band represented fish originating from the Garonne river basin and returning to the Garonne river basin (autochthonous fish). The four lines at the bottom indicated the origins of the allochthonous fish entering the Garonne river basin. Lines above the light grey band indicated the destinations of Garonne strayers in the Atlantic area. Lines were proportional to the net nitrogen import. River basins on the right were ordered by latitude, with the exception of the Garonne river basin.

369x208mm (96 x 96 DPI)

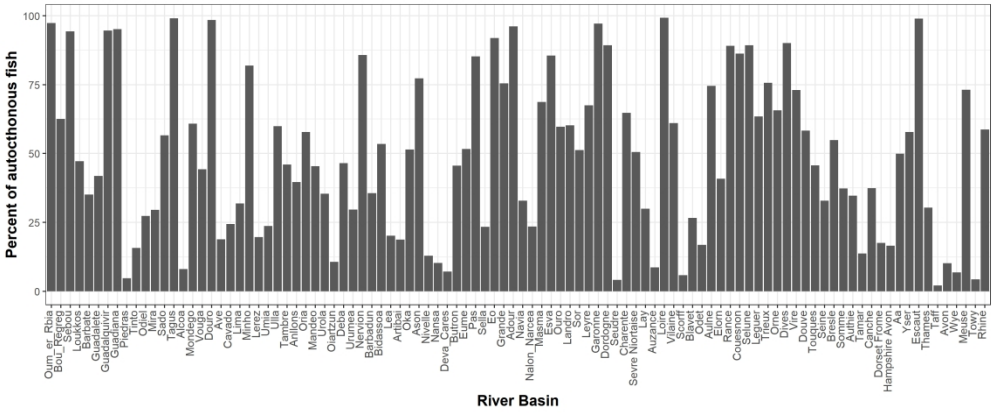

Figure 3. Contribution of the autochthonous fish (in %) to the total import of nitrogen over the period 1900-1930 in the river basins colonized by shads in the GR3D physical environment. The remaining percent was for inputs derived from strayers coming from other rivers. River basins were ordered along a latitudinal gradient from Morocco to Germany.

304x127mm (300 x 300 DPI)

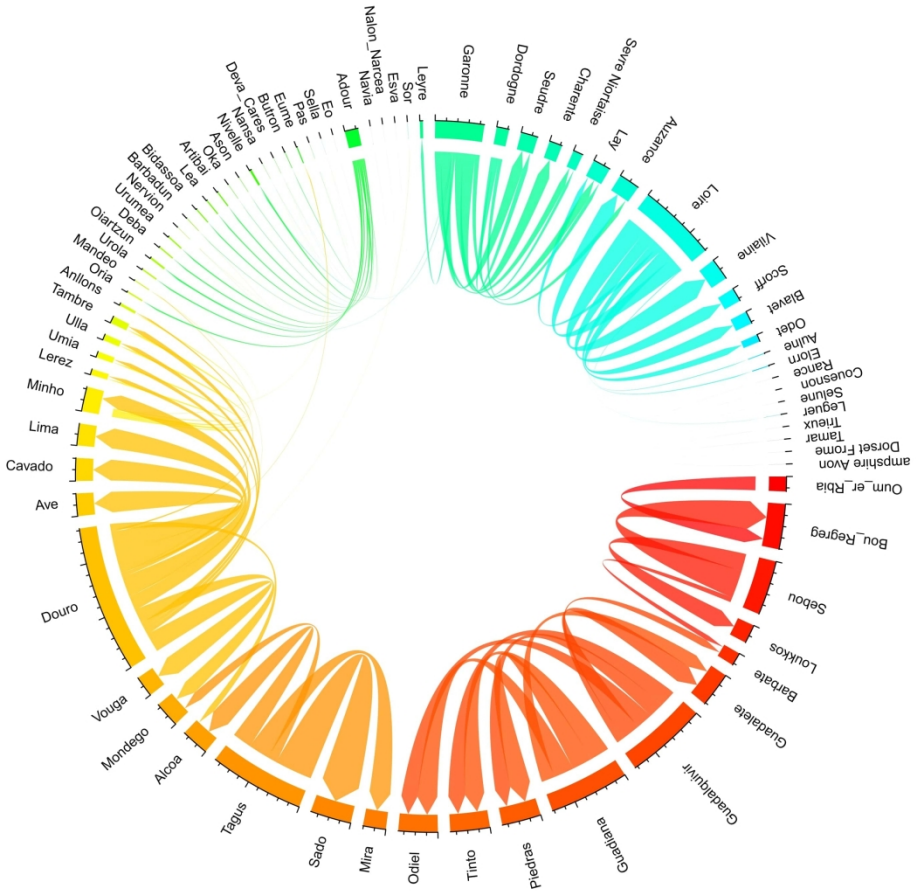

Figure 4. Interdependencies among river basins in nitrogen supplies provided by allis shad allochthonous fish straying from one to another river (KgN) over the period 1900-1930. Each intermediate tick mark increases by 800 kgN, starting from 0. River basins were ordered clockwise along a latitudinal gradient, ranging from the Oum Er-Rbia river basin at the southern edge of the distribution in Morocco (red) to the Avon river basin at the northern edge of the distribution in the U.K (blue). To ease the reading, only the nitrogen supplies provided by allochthonous fish contributing more than 10% of the total nutrient subsidies imported in each river basin were represented in the figure. The magnitude and flow of each relationship were indicated by arrow size and direction, respectively. A latitudinal color gradient was used to distinguish among arrows from different basins. The contribution of autochthonous fish was not represented in the Chord Diagram.

1058x1164mm (72 x 72 DPI)

Appendix 1: Detailed description of the GR3D model and its physical environment

Overall model description

GR3D (Global Repositionning Dynamics for Diadromous fish Distribution) was developed to assess the repositioning of diadromous species under climate change over large spatial and temporal scales. It was written in Java using the "SimAqualife" software framework especially designed for spatialized and individual-based simulations of aquatic life movements. GR3D is an individual-based stochastic model. It integrates and combines population dynamics with explicit formulation of key life-history processes and climatic requirements.

GR3D was developed to cover the entire life cycle of any diadromous fish species. The model was divided into six sub-models consistent with the life cycle events and processes of any diadromous species *i.e.* reproduction, growth, survival, downstream migration, maturation, dispersal and upstream migration. A set of 42 parameters is associated to the different processes with parameter values obtained either from literature, expert elicitation or calibration (Table A1). The model was first parameterized for Allis shad (*Alosa alosa*) in Western Europe.

Population dynamics within the model

Individuals reproduce every spring in a river basin and produce juveniles. The number of recruits R_j produced by the spawning stock S_j in a given basin j is assumed to follow a Beverton and Holt stock-recruitment relationship of parameters α_j and β_j (BH S-R) (eq1. (A1)).

The recruitment r_0 is linked to species fecundity (α) and depends on the number of spawners *Sj* in the spawning basin *j*. The BH S-R included in GR3D differs from the traditional BH S-R in two aspects:

(1) An "Allee effect" is included within the reproductive process to simulate difficulties to settle a functional population with limited numbers of individuals in new habitats. Depensation strength (i.e., the number of spawners that effectively participate in reproduction) is depending on the river basin surface (wa_j) through the η and θ parameters. The intensity of the "Allee Effect" is positively correlated to parameter η and negatively correlated to parameter θ.

(2) The mortality from eggs to recruits is modeled as a function of temperature and spawning basin surface. The non-density-dependent mortality is a function of temperature (α_j and β_j). The relationship between the non-density mortality and the water temperature follows a dome-shape curve. Thus, T_{minR} and T_{maxR} define the range in which temperature ensures recruitment and egg survival, with an optimal survival at T_{optR}. The density-dependent mortality of the BH S-R depends on basin surface (through a population parameter λ) to consider resource limitations in small basins.

$$R_j = \frac{\alpha_j S_j \frac{1}{1+e^{\left(-\ln(19)\frac{S_j-\eta/\theta.wa_j}{\eta.wa_j-\eta/\theta.wa_j}\right)}}}{\beta_j + S_j \frac{1}{1+e^{\left(-\ln(19)\frac{S_j-\eta/\theta.wa_j}{\eta.wa_j-\eta/\theta.wa_j}\right)}}} \qquad \text{eq1. (A1)}$$

After the reproduction, the probability of spawners to survive is given through the Sp_{sp} parameter. For semelparous species dying after reproduction, this probability is set to a low value of 0.1.

Growth of individuals is modeled as a Von Bertalanffy growth function. An effect of water temperature (T °C) on the growth coefficient K is introduced in the process through a dome-shape relationship as it was described above for reproduction (eq2.(A1)). Thus, at $T_{optGrow}$, the growth coefficient is optimum ($K_{optGrow}$) and becomes null when T is out of the range defined by $T_{minGrow}$ and $T_{maxGrow}$:

$$k = k_{optGrow}\frac{(T - T_{minGrow})(T - T_{maxGrow})}{(T - T_{minGrow})(T - T_{maxGrow})(T - T_{optGrow})} \quad \text{eq2.(A1)}$$

After spending several years at sea, ripe individuals (here an individual is assumed to be mature when it reaches its size at maturity, L_{mat}) start their spawning migration and enter a river basin to reproduce. The upstream migration included an original dispersal process which is designed as a three-stage process with (1) emigration, (2) transfer and (3) settlement phases.

(1) During the emigration phase, individuals have a probability to adopt a homing behavior (p_{hom}) or a straying behavior (1- p_{hom}), with p_{hom} defined as a model parameter.

(2) During the transfer phase, individuals that do not adopt a straying behavior, simply migrate to their natal river. For strayers, the probability to migrate in each river basin is assumed to be a function of its accessibility. Accessibility is assumed to depend on dispersal distance between the natal basin and the new basin *j*. Then, relatively to an individual, a weight is calculated for each river basin using a logit function with some parameters defined as model parameters. Assuming that the individuals may not find

a basin and simply die during transfer, a virtual 'death basin' with a fixed weight ($W^{deathBasin}$) is also introduced. The probability to choose each river basin (including the death one) was obtained by standardizing all the weights so that their sum equals 1. The choice of a destination basin is then modeled by a simple multinomial process.

(3) During the settlement phase, individuals enter in the destination basin, survive if conditions are suitable and reproduce if they find mating requirements.

The dispersal was then modeled by eq3. (A1):

$$w_{j_1 \to j_2} = \frac{1}{1 + e^{\alpha_0 + \alpha_1 \cdot \frac{(D_{j_1 \to j_2} - \mu_D)}{\sigma_D}}}$$

eq3. (A1)

where $D_{j_1 \to j_2}$ is the distance between the departure and destination basins, α_0 and α_1 are the kernel parameters, μ_D and σ_D are the mean and standard deviation for the inter-basin distances.

At each time step, the probability of each individual to survive is estimated regarding its location along the land-sea continuum. The seasonal survival probability (Sp_{sea}) is based on the annual mortality coefficients Z_{sea} and Z_{river} which depend on age and water temperature.

Table A1. Description of the GR3D parameters with nominal values for the 42 parameters included in the model. A red asterisk marked parameters modified from the original GR3D version (Rougier et al. 2014). New parameters values were obtained from either literature or offline calibration.

Parameter name	Description	Nominal value
Reproduction		
repSeason	Season of the reproduction	Spring
Δt_{rec}	Assumed age of juvenile produced by the reproduction (year)	0.33
η	Parameter to relate $S_{95,j}$ and the surface of a spawning place (ind./km^2)	2.4
θ	Ratio between $S_{95,j}$ and $S_{50,j}$ in each spawning place	1.9
*α	Fecundity of the species (eggs/ind.)	270 000
$surv_{optRep}$	Optimal survival rate of an individual from eggs to the age Δt_{rec}	$1*7^{-3}$
*T_{minRep}, T_{optRep}, T_{maxRep}	Water temperature (°C) regulating survival of an individual from eggs to the age Δt_{rec}	[9.3, 20.8, 31]$^{(a)}$
λ	Parameter to relate c_j and the surface of a spawning place	$4.1*10^{-4}$
σ_{rep}	Standard deviation of log-normal distribution of the recruitment	0.2
Sp_{sp}	Survival probability of spawners after reproduction	0.1
Downstream migration		
downMigAge	Age of individual when it runs toward the sea (year)	0.33
downMigSeason	Season of the run toward the sea	Summer
Growth		
L_{inf}	Initial length of juveniles in estuary (cm)	2
$\sigma_{\Delta L}$	Standard deviation of log-normal distribution of the growth increment	0.2
*L_∞	Asymptotic length of an individual (cm)	70$^{(b)}$
$T_{minGrow}$, $T_{optGrow}$, $T_{maxGrow}$	Water temperature (°C) regulating the growth	[3, 17, 26]
*$k_{optGrowFemale}$	Optimal growth coefficient for females	0.3236 $^{(b)}$
*$k_{optGrowMale}$	and males (cm/season)	0.2141$^{(b)}$
Survival		
Z_{sea}	Annual mortality coefficient at sea (year^{-1})	0.4
H_{riv}	Annual mortality (different from natural) coefficient in river (year^{-1})	0
*$T_{minSurvRiv}$, $T_{optSurvRiv}$, $T_{maxSurvRiv}$	Water temperature (°C) regulating survival of individuals in river	[10.7, 17, 25.7]$^{(c)}$
$surv_{optRiv}$	Optimal natural survival rate of individuals in river (year^{-1})	1
Maturation		
*$L_{matFemale}$	Length at the first maturity (cm)	55 $^{(a)}$

*$L_{matMale}$		40 [(a)]
Upstream migration		
upMigAge	Age of an individual when it runs toward the river (year)	
upMigSeason	Season of the return of spawners in river for spawning	Spring
p_{hom}	Probability to do natal homing behavior	0.75
α_{const}, α_{dist}, α_{TL}, α_{WA}	Parameters of the logit function used to determine the weight of each accessible basin for dispersers/strays	-2.9, 19.7, 0, 0
$D_{j\text{-}birhtPlace}$, $\sigma_{j-birthPlace}$, TL, σ_{TL}, WA, σ_{WA}	Mean and standard deviation used for standard core values in the logit function	300, 978,-,-,-, -
$w^{deathBasin}$	Weight of the death basin used to introduce a mortality of dispersers/strays	[0.2–0.6]

[(a)] Computed from offline calibration, [(b)] Modified from Jatteau *et al.*, 2017, [(c)] Modified from Paumier *et al.*, 2019

Description of the physical environment

The physical environment of the model is composed of a set of both river and sea basins connected to each other and spatially geo-referenced. Both river and sea basins are characterized by seasonal temperature time series (T°C), while river basins are also characterized by their surface (km^2). The physical environment included 135 river basins along the European Atlantic coast, ranging from the south of Portugal to the British Isles and Norway (Fig. A1).

Fig. A1. Map of the 135 European river basins implemented into the GR3D physical environment. The 13 rivers basins used for model partial validation are represented in light red. Sources: European Commission. Joint Research Centre. Institute for Environment and Sustainability, American Geophysical Union. Projection: WGS 84

Description of the data used to compare model estimates and observations of allis shad abundances in the 13 well-studied rivers.

Data regarding allis shad spawner abundance were derived from several sources.

For the Lima, Minho and Adour rivers, abundances were estimated from annual commercial fishery landings (e.g. Mota et al. 2015).

For the Lima and Adour rivers, landings were given in kilograms of fish caught, so biomass was divided by an average mass of fish; W = 2.1 kg in the Lima, and W = 1.7 kg in the Adour respectively)(ICES, 2015) to broadly estimate fish abundances in both rivers.

For the Garonne and the Charente rivers, abundances were derived from the counting of spawning events. During the reproduction, shads exhibit a circular and noisy movement; herafter called 'splash' at the water surface, that can be recorded to monitor the spawning activity (Mennesson-Boisneau 1990). The number of 'splashes' recorded is often used as a good estimator to assess the spawning stock.

For the other rivers, a video-counting system at fishways was used to assess the spawning stock. Video-counting provide reliable estimates of migrating adults, because systems are usually located downstream of the main spawning grounds but some fish may not cross the barriers and therefore are not counted by the device (P.Jatteau, pers. obs).

For several rivers, data do not discriminate between *A. fallax* and *A. alosa* and provide a net annual balance between adults migrating upstream and juveniles migrating downstream.

References

ICES. 2015. Report of the Workshop on Lampreys and Shads (WKLS), 27-29 November 2014, Lisbon, Portugal. ICES CM 2014/SSGEF:13. 206 pp.

European Commission. Joint Research Centre. Institute for Environment and Sustainability. 2007. A pan-European river and catchment database. Publications Office, LU. Available from https://data.europa.eu/doi/10.2788/35907.

Jatteau, P., Drouineau, H., Charles, K., Carry, L., Lange, F., and Lambert, P. 2017. Thermal tolerance of allis shad (*Alosa alosa*) embryos and larvae: Modeling and potential applications. Aquat. Living Resour. **30**: 2. doi:10.1051/alr/2016033.

Lehner, B., Verdin, K.L., and Jarvis, A. 2008. New global hydrography derived from spaceborne elevation data. doi:10.1029/2008EO100001.

Mennesson-Boisneau, C. 1990. Migration, répartition, reproduction et caractéristiques biologiques des aloses (Alosa sp.) dans le bassin de la Loire.

Mota, M., Bio, A., Bao, M., Pascual, S., Rochard, E., and Antunes, C. 2015. New insights into biology and ecology of the Minho River Allis shad (Alosa alosa L.): contribution to the conservation of one of the last European shad populations. Rev. Fish Biol. Fish. **25**(2): 395–412. doi:10.1007/s11160-015-9383-0.

Paumier, A., Drouineau, H., Carry, L., Nachón, D.J., and Lambert, P. 2019. A field-based definition of the thermal preference during spawning for allis shad populations (Alosa alosa). Environ. Biol. Fishes **102**(6): 845–855. doi:10.1007/s10641-019-00874-7.

Rougier, T., Drouineau, H., Dumoulin, N., Faure, T., Deffuant, G., Rochard, E., and Lambert, P. 2014. The GR3D model, a tool to explore the Global Repositioning Dynamics of

Diadromous fish Distribution. Ecol. Model. **283**: 31–44. doi:10.1016/j.ecolmodel.2014.03.019.